Instant nano-hydroxyapatite: a continuous and rapid hydrothermal synthesis†

Aqif A. Chaudhry,[a] Saba Haque,[a] Suela Kellici,[a] Paul Boldrin,[a] Ihtesham Rehman,[b] Fazal A. Khalid[c] and Jawwad A. Darr*[a]

Received (in Cambridge, UK) 21st December 2005, Accepted 6th April 2006
First published as an Advance Article on the web 2nd May 2006
DOI: 10.1039/b518102j

Nano-particle hydroxyapatite (HA) rods, were rapidly synthesised using a three pump continuous hydrothermal process (using a water feed at up to 400 °C and at 24 MPa): the product was obtained as a highly crystalline and phase pure material, without the need for an ageing step or subsequent heat treatment.

Synthetic hydroxyapatite [HA, $Ca_{10}(PO_4)_6(OH)_2$], is a bioactive material that is chemically similar to biological apatite, the mineral component of bone.[1] Indeed, human bone is a natural composite comprising of nano-apatite rods (which are <100 nm) arranged in lamellae and bound to collagen.[2] Thus, synthetic HA is of interest as a biocompatible phase reinforcement in biomedical composites, for filling bulk bone defects and for coatings on metal implants.[3] HA and other calcium phosphates (calcium deficient hydroxyapatite, CDHA) are also of interest as components in injectable bone cements; controlling particle properties (*e.g.* size and shape) is often used to modulate cement setting behaviour.[4]

HA powders and coatings can be synthesised using a number of methods including sol-gel processing,[5] co-precipitation,[6,7] emulsion techniques,[7–9] batch hydrothermal processes,[10–14] mechano-chemical methods[15] and chemical vapour deposition.[16] The disadvantages of these methods include the following; they often require very precise control over reaction conditions,[5–16] require expensive starting materials[5,16] or large amounts of toxic organic solvents,[7–9] or they are usually time consuming.[5–11] For example, in wet chemical syntheses of HA, a maturation step (>18 h), followed by a heat treatment of 650 °C, is required.[6,7,17] Failure to allow sufficient maturation, gives a phase separated product upon heat treatment, which can adversely affect biological properties *in vivo*. Furthermore, the aforementioned synthesis approaches give little or no control over HA particle characteristics (*i.e.* particle size, agglomeration surface area, shape, *etc.*).[18,19]

Batch hydrothermal syntheses of HA as reported in the literature are normally conducted in the range 60–150 °C for up to 24 h to yield crystalline HA rods that are usually agglomerated.[10–14] Such batch reactions can include organic templating agents,[11,13] which are surface bound and therefore potentially unsuitable for biomedical applications as they may elicit an adverse response *in vivo*. To gain a better understanding of the factors that produce particles with the desired properties, current synthesis methods are essentially too slow and unpredictable. Thus, there is interest in developing faster synthesis techniques for synthetic apatites that allow a greater degree of control over particle properties.

Continuous hydrothermal syntheses have recently gained interest as a fast and controllable method for producing inorganic nano-materials (particles <500 nm).[20–23] Previous examples include the rapid synthesis of nano-materials that normally require long synthesis times or that are difficult to manufacture using more conventional methods.[20–23] Thus, we postulated that the rapid nucleating and crystallising environment within a hydrothermal flow reactor may facilitate accelerated synthesis of crystalline nano-apatites in a single step.

In this report, we describe the rapid, single step synthesis of crystalline nano-particle hydroxyapatite rods (Fig. 1) in a continuous hydrothermal flow system (using water at <400 °C and 24 MPa pressure). This process (see diagram in Fig. 2) has many advantages; it does not use any organic templating agents[11,13] and effectively reduces the time required for maturation of the reagents from over 18 h (under standard conditions) to a few seconds.[6,7] In our process, basic solutions of calcium nitrate and ammonium phosphate, respectively, were pumped to meet at a "Tee" piece mixer (T in Fig. 2). This initial mixture was then brought to meet a superheated water feed in a counter current reactor (R), whereupon, rapid ageing occurred.‡,§ The apatite suspension was collected at the exit of the back-pressure regulator (B) after first passing though the in-line cooler (C) and a 7 μm filter (F). The collected particles were centrifuged and the wet solids were freeze-dried prior to further analyses.

Transmission electron microscope (TEM) images of the powders synthesised with superheated water at 200 °C [denoted as sample HA(200)],‡ revealed small agglomerates.† TEM images for HA(300),‡ showed well defined rods of *ca.* 15 × 65 nm (aspect ratio *ca.* 4.3).† The TEM image for HA(400),‡ (Fig. 1) revealed well defined crystalline rods of *ca.* 140 × 40 nm (aspect ratio *ca.* 3.5). A selected area diffraction pattern for sample HA(400), suggested the material was polycrystalline (inset on Fig. 1(b)).

BET surface area measurements for CDHA(200), HA(300) and HA(400) were measured at *ca.* 88, 100 and 39 $m^2\ g^{-1}$, respectively. The control sample, CDHA(400)¶ (made under acidic conditions) had a surface area of 67 $m^2\ g^{-1}$. Despite sample CDHA(200) being the least crystalline, it possesses a slightly lower surface area

[a]*Department of Materials, Queen Mary University of London, Mile End Road, London, UK E1 4NS. E-mail: j.a.darr@qmul.ac.uk; Fax: +44 208 9819804; Tel: +44 207 8825191*
[b]*IRC in Biomedical Materials, Queen Mary University of London, Mile End Road, London, UK E1 4NS*
[c]*Faculty of Metallurgy and Materials Engineering, Ghulam Ishaq Khan Institute of Engineering Sciences and Technology, Topi 23460, District Swabi, NWFP, Pakistan*

† Electronic supplementary information (ESI) available: TEM images FTIR spectra, XRD pattern and TGA-DSC plots. See DOI: 10.1039/b518102j

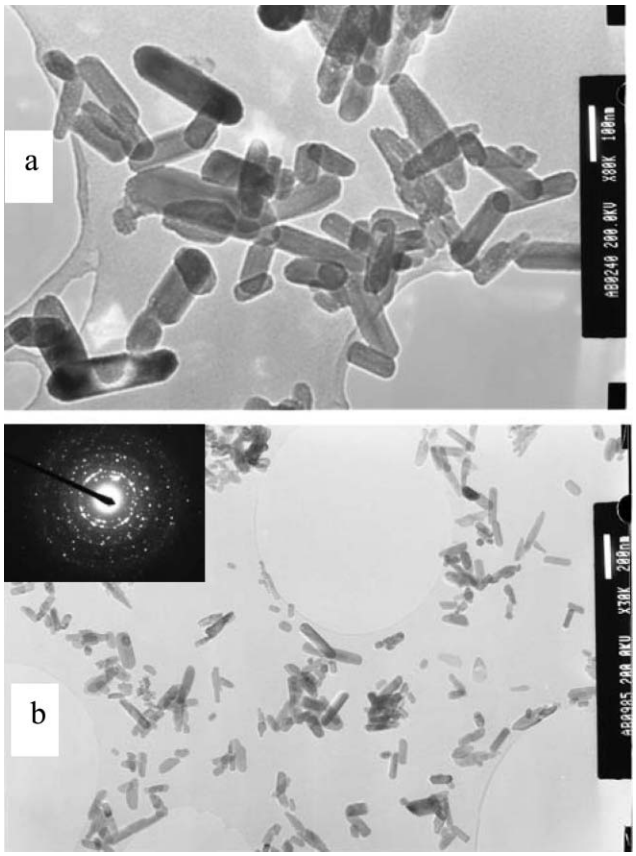

Fig. 1 Transmission electron microscope images of hydroxyapatite nano-rods for sample HA(400) made using superheated water at 400 °C and 24 MPa in the hydrothermal flow system; (a) magnification ×80k (bar = 100 nm), and for (b) magnification ×30k (bar = 200 nm). Inset is the selected area diffraction pattern.

than HA(300), possibly due to the former being more agglomerated. In contrast, "as precipitated" amorphous HA made at room temperature was reported elsewhere to possess a surface area of 90 $m^2\ g^{-1}$ after oven-drying and 113 $m^2\ g^{-1}$ after freeze-drying.[7]

The crystallinity of the nano-powders was assessed by both X-ray powder diffraction (XRD) and Fourier transform infrared (FTIR) spectroscopy. The broad XRD pattern for CDHA(200) suggests an apatite-like structure (Fig. 3(iv)). XRD patterns for HA(300), CDHA(400)¶ and HA(400), respectively, showed a good match to phase pure HA [compared to JCPDS pattern 09-0432 (I)-Hydroxyapatite, *syn*-$Ca_5(PO_4)_3(OH)$].[24] The XRD peaks became increasingly sharper and well resolved, with increasing synthesis temperature, the CDHA(400) being noticeably less sharp than the HA(400) sample. Application of the Scherrer equation to the XRD half peak widths, suggested a crystal size of 12, 17 and 25 nm for HA(300), CDHA(400) and HA(400), respectively.[25]

FTIR spectroscopy data† revealed peaks at 3570 and 633 cm^{-1} (corresponding to stretching and librational mode of the hydroxyl group in HA, respectively) which grew stronger and sharper with increasing temperature. The intensity of a peak at 1639 cm^{-1}, corresponding to the bending mode for lattice water, was observed to decrease with increasing synthesis temperature. This suggested that loosely bonded OH^- groups became more incorporated into the lattice with an increase in temperature. Peaks at 1453 and 1414 cm^{-1} correspond to the stretching modes, respectively, of some substituted carbonate in the HA.‖,[26] Peaks at 1096 and 1031 cm^{-1} correspond to the P–O asymmetric stretching mode of phosphate, whilst the peak at 961 cm^{-1} corresponds to the P–O symmetric stretch. Peaks at 603, 567 and 466 cm^{-1} correspond to O–P–O bending modes. An increase in intensity and sharpness of these peaks with temperature, indicates an increase in crystallinity of HA.[24]

Thermal behaviour of the samples was assessed using simultaneous thermal analysis (STA) from room temperature (RT) to 1200 °C.† The thermogravimetric analysis (TGA) weight loss plot for sample HA(400) shows three overlapping regions of weight loss at 30–170 °C (1.2 wt% loss of weakly adsorbed water), 170–595 °C (1.9 wt% loss of lattice water) and 595–1014 °C (1.1 wt% of CO_2), respectively. Thereafter, there is a sudden weight loss (5.7 wt%) up to 1200 °C to give a total weight loss of 9.9 wt%.[27] Above 1014 °C, phase decomposition occurred.

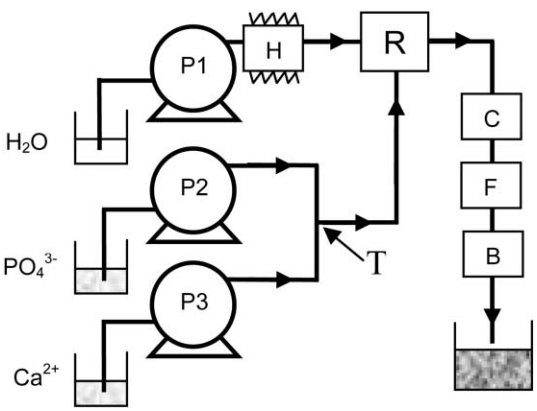

Fig. 2 Scheme of the three-pump (P1, P2 and P3) hydrothermal flow system used for the synthesis of nano-HA. Key: P = pump, H = heater, C = cooler, F = filter, B = back-pressure regulator, R = reactor, T = "Tee" piece mixer.

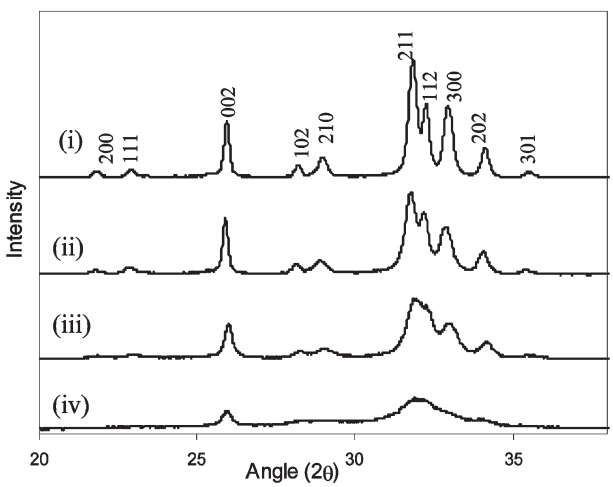

Fig. 3 X-Ray powder diffraction patterns of the nano-apatite powders made in the hydrothermal flow system using superheated water for samples (i) HA(400), (ii) CDHA(400), (iii) HA(300) and (iv) CDHA(200), respectively.

Differential scanning calorimetry (DSC) data for HA(400) was rather featureless, revealing only a broad endotherm centred at *ca.* 70 °C. In contrast, the STA data for HA(300) show very smooth weight loss up to 1011 °C (8.2 wt% loss at this temperature) with only one endotherm clearly observed in the DSC plot at *ca.* 70 °C. Sample CDHA(200) showed the largest weight loss by 1008 °C (total loss = 16.0 wt%). The DSC data for CDHA(200) and for the control sample CDHA(400), revealed endotherms centered at 750 and 770 °C, respectively, which were not observed in the DSC plots for sample HA(300) or HA(400). We confirmed using XRD of CDHA(200) heated to 800 °C for 2 h, that this transformation was due to the (calcium deficient) apatite forming into a mixture of β-TCP (tri-calcium phosphate, whitlockite) and HA, rather than being stable.[28],† This suggested that CDHA(200) was calcium deficient [as was sample CDHA(400)].†,¶,**

In conclusion, crystalline, phase pure nano-hydroxyapatite and calcium deficient apatite were synthesised in a continuous hydrothermal synthesis system. The versatility of this method should allow homogenous doping of biologically beneficial ions (*e.g.* Si or Na ions) into the apatite structure. Indeed, our recent unpublished results are promising in this regard; the results of these endeavours will be reported in due course.

EPSRC is thanked for funding an EPSRC Advanced Research Fellowship entitled "Next Generation Biomedical Materials Using Supercritical Fluids" (JAD; grant GR/A11304) and an industrial case award (PB). The Higher Education Commission (HEC), Government of Pakistan is thanked for a scholarship (AAC). Johnson Matthey is also thanked for supporting the industrial case award (PB). Dr E. Lester and Dr P. Blood (University of Nottingham) are thanked for useful discussions.

Notes and references

‡ Materials and methods: Diammonium hydrogen phosphate, [$(NH_4)_2HPO_4$, 98.3%] and calcium nitrate tetrahydrate [$Ca(NO_3)_2{\cdot}4H_2O$, 99.0%] were supplied by Sigma-Aldrich Chemical Company (UK). Ammonium hydroxide solution (NH_4OH, $\geqslant$30% w/w) supplied by VWR International (UK) was used to adjust the pH. 10 MΩ deionised water was used in all reactions. 0.05 M diammonium hydrogen phosphate solution and 0.0835 M calcium nitrate solutions were used (Ca : P molar ratio: 1.67). The pH of both the solutions prior to the reaction was kept above pH 10. 1.0 ml and 12.0 ml of ammonium hydroxide were added to calcium nitrate (500 ml) and diammonium hydrogen phosphate solutions (500 ml), respectively. Calcium nitrate and diammonium hydrogen phosphate solutions were pumped at 5 ml min^{-1} and water was pumped through the heater at 10 ml min^{-1}. Samples were labelled according to the temperature of the superheated water used, thus, samples prepared at 300 and 400 °C with a Ca : P ratio of 1.67, were labelled HA(400), and HA(300), respectively. The sample at 200 °C was labelled CDHA(200), as it was found to be calcium deficient.

§ Experiments were conducted using a modified flow reactor design to that reported previously.[20–23] The new system added a third Gilson 305 pump and a Tee piece (for premixing the Ca and P sources before meeting the superheated water feed) and a new counter-current mixing reactor that reduces blockages.[29] The pumps used 10 ml Ti pump-heads and most of the tubing and fittings were 1/8″ 316SS Swagelok™, except the counter-current reactor, which was 3/8″.[29,30] After collection, the particles were centrifuged at 4500 rev s^{-1} for 3 min. The solids were frozen in liquid nitrogen and then freeze-dried for 18 h at 1 $\times 10^{-4}$ mbar.

¶ A fourth control experiment was conducted using a similar method, with the superheated water feed at 400 °C, (under acidic rather than basic conditions) and a Ca : P ratio of 1 : 1 [denoted as sample CDHA(400) as it was later found to be calcium deficient]. 0.05 M $(NH_4)_2HPO_4$ and 0.05 M $Ca(NO_3)_2{\cdot}4H_2O$ solutions had a pH of 8.5 and 5.5 respectively. The suspension exiting the hydrothermal flow system had a pH of 6.

‖ The HA contains *ca.* 1.5 wt% carbonate substitution (based on TGA weight loss of CO_2) for phosphate in the lattice (known as B-type). This was not unexpected as the reagent solutions were not degassed to remove dissolved carbon dioxide, which ultimately gives carbonate.[26] The peak at 872 cm^{-1} (bending mode of the CO_3^{2-}), also becomes sharper as the temperature is increased.

** Equipment and techniques: Freeze-drying was performed using a VirTis AdVantage Freeze Dryer, Model 2.0 ES. FTIR spectra were collected using a Nicolet FTIR 8700 spectrometer fitted with a photoacoustic sampler (MTech PAS Cell), with 4 cm^{-1} spectral resolution, averaging 256 scans. Simultaneous TGA and DSC were carried out using a Polymer Labs STA 1500 (heating rate 10 °C min^{-1}). BET surface area measurements (using N_2 gas), were performed on a Micromeritics Gemini analyser; powders were degassed at 200 °C for 2 h prior to analyses. A JEOL 2010 Transmission Electron Microscope (200 kV accelerating voltage) was used for generating images of particles. XRD data were collected on a Siemens D5000 X-Ray diffractometer using Cu-Kα radiation (λ = 0.15418 nm) over the 2θ range 5–110° with a step size of 0.02° and a count time of 10 s.

1 A. E. Porter, S. M. Best and W. Bonfield, *J. Biomed. Mater. Res. A*, 2004, **68**, 133.
2 P. Fratzl, H. S. Gupta, E. P. Paschalis and P. Roschger, *J. Mater. Chem.*, 2004, **14**, 2115.
3 L. L. Hench, *J. Am. Ceram. Soc.*, 1998, **81**, 1705.
4 M. P. Ginebra, F. C. M. Driessens and J. A. Planell, *Biomaterials*, 2004, **25**, 3453.
5 A. Bigi, E. Boanini and K. Rubini, *J. Solid State Chem.*, 2004, **177**, 3092.
6 Y. X. Pang and X. Bao, *J. Eur. Ceram. Soc.*, 2003, **23**, 1697.
7 M. J. Phillips, J. A. Darr, Z. B. Luklinska and I. Rehman, *J. Mater. Sci.: Mater. Med.*, 2003, **14**, 875.
8 M. J. Phillips, Ph. D. Thesis, 2005, Queen Mary University of London.
9 G. K. Lim, J. Wang, S. C. Ng, C. H. Chew and L. M. Gan, *Biomaterials*, 1997, **18**, 1433.
10 C. R. Kothapalli, M. Wei, R. Z. LeGeros and M. T. Shaw, *J. Mater. Sci.: Mater. Med.*, 2005, **16**, 441.
11 Y. Wang, S. Zhang, K. Wei, N. Zhao, J. Chen and X. Wang, *Mater. Lett.*, 2006, **60**, 1484.
12 R. E. Riman, W. L. Suchanek, K. Byrappa, C. Chen, P. Shuk and C. S. Oakes, *Solid State Ionics*, 2002, **151**, 393.
13 F. Zhang, Z. Zhou, S. Yang, L. Mao, H. Chen and X. Yu, *Mater. Lett.*, 2005, **59**, 1422.
14 J. Liu, X. Ye, H. Wang, M. Zhu, B. Wang and H. Yan, *Ceram. Int.*, 2003, **29**, 629.
15 S. Rhee, *Biomaterials*, 2002, **23**, 1147.
16 J. A. Darr, Z. X. Guo, V. Raman, M. Bououdina and I. U. Rehman, *Chem. Commun.*, 2004, **6**, 696.
17 S. Kim, H. Ryu, H. Shin, H. S. Jung and K. S. Hong, *Mater. Chem. Phys.*, 2005, **91**, 500.
18 H. Arce, M. L. Montero, A. Sáenz and V. M. Castano, *Polyhedron*, 2004, **23**, 1897.
19 L. Y. Cao, C. B. Zhang and J. F. Haung, *Mater. Lett.*, 2005, **59**, 1902.
20 Y. Hakuta, H. Ura, H. Hayashi and K. Arai, *Mater. Chem. Phys.*, 2005, **93**, 466.
21 K. Sue, K. Kimura and K. Arai, *Mater. Lett.*, 2004, **58**, 3229.
22 A. Cabanas, J. A. Darr, E. Lester and M. Poliakoff, *J. Mater. Chem.*, 2001, **11**, 561.
23 A. Cabanas, J. A. Darr, E. Lester and M. Poliakoff, *Chem. Commun.*, 2000, 901.
24 S. Koutsopoulos, *J. Biomed. Mater. Res.*, 2002, **62**, 600.
25 E. Bouyer, F. Gitzhofer and M. I. Boulos, *J. Mater. Sci.: Mater. Med.*, 2000, **11**, 523.
26 E. Landi, G. Celotti, G. Logroscino and A. Tampieri, *J. Eur. Ceram. Soc.*, 2003, **23**, 2931.
27 W. L. Suchanek, P. Shuk, K. Byrappa, R. E. Riman, K. S. TenHuisen and V. F. Janas, *Biomaterials*, 2002, **23**, 699.
28 T. I. Ivanova, O. V. Frank-Kamenetskaya, A. B. Kol'tsov and V. L. Ugolkov, *J. Solid State Chem.*, 2001, **160**, 340.
29 E. Lester, P. Blood, J. Denyer, D. Giddings, B. Azzopardi and M. Poliakoff, *J. Supercritic. Fluids*, 2006, **37**, 209.
30 P. J. Blood, J. Denyer, B. J. Azzopardi, M. Poliakoff and E. Lester, *Chem. Eng. Sci.*, 2004, **59**, 2853.

